Angular distributions of Auger transitions of N_2 to dissociative final states

A. K. Edwards, Q. Zheng, R. M. Wood, and M. A. Mangan
Department of Physics and Astronomy, University of Georgia, Athens, Georgia 30602
(Received 11 September 1996; revised manuscript received 18 February 1997)

The angular distribution of the 360.2-eV Auger transition in N_2, which is attributed to an $N_2^{2+}\,{}^1\Pi_g$ final state, is measured and calculated. Calculations predict a sharper distribution than what is measured. The angular distribution of the 363.5-eV Auger transition, attributed to an $N_2^{2+}\,{}^1\Pi_u$ final state, is nearly isotropic in the laboratory frame. This is believed to be caused by metastable vibrational levels of the final state. The final state of the 358.7-eV transition was found to be nondissociative, and its angular distribution could not be measured by our experimental technique. The peak in the N^+ fragment-ion spectrum at about 3.9 eV is assigned to the $^3\Sigma_g^-$ dissociative state of N_2^{2+}. [S1050-2947(97)08806-9]

PACS number(s): 33.80.Eh, 34.80.Gs

I. INTRODUCTION

Two recent publications from this laboratory [1,2] described the measurements of the angular distribution of the 362.5-eV Auger transition in N_2, and a procedure for calculating the angular distribution of Auger transitions of homonuclear diatomic molecules. In order to determine the angular distribution of the Auger electrons for randomly oriented molecules, it is necessary to know the orientation of the internuclear axis of the molecule undergoing the transition. This is done by means of a coincidence experiment. Following the Auger transition, the doubly ionized molecular ion can be left in a dissociative state where each fragment ion escapes with energies that are in the range of 1–10 eV. Typically, the dissociation time is short compared to the rotation time. As a consequence, the path of the fragment ions is approximately along the line of the internuclear axis at the time of the Auger transition. One detector is placed at a selected angle relative to the incident-beam direction, and detects fragment ions. Another detector is placed at some other angle relative to the first, and measures an electron ejected by a selected Auger transition.

Eberhardt *et al.* [3] measured Auger electrons in coincidence with fragment ions from N_2 as a means of identifying the final molecular-ion states. The charge states and kinetic energies of the fragments were determined, and comparisons were made to predictions based on the potential-energy curves of Thulstrup and Anderson [4], and the calculations of Ågren [5]. The newer potential-energy curves of N_2^{2+} calculated by Wetmore and Boyd [6], Olsson, Kindvall, and Larsson [7], and O'Neil [8] are used in analyzing the present results and in our calculations that predict the angular distributions.

The dissociative ionization of N_2 by fast ions leading to the coincident detection of two N^+ fragments was reported by Edwards and Wood [9]. They argued that the primary contributions to the $N^+ + N^+$ yield was valence-shell ionization rather than inner-shell ionization and its subsequent Auger transition. Thus there is no correlation in intensities between the Auger spectrum and the N^+ spectrum. Lundqvist *et al.* [10] developed an experimental procedure to record the N^+ spectrum free of thermal broadening. They were able to detect vibrational states of N_2^{2+} that are metastable toward dissociation, and have lifetimes up to a few microseconds. These metastable states rotate many times prior to dissociation, and contribute a uniform angular distribution to our measurements.

This work selects out those dissociation products that arise from selected Auger transitions at 363.5, 360.2, and 358.7 eV [11]. These are the strong transitions displayed in the Auger spectrum, and are known by the labels B-3, B-5, and B-6, respectively. The Auger transitions at 362.5 eV, measured earlier [1], is the B-4 peak. The two lowest-energy states of N_2^{2+} lie in deep potential wells and are not dissociative. The B-1 and B-2 transitions are assumed to be transitions to these states, and were not investigated.

II. EXPERIMENTAL PROCEDURE

The experimental procedure was reported in Zheng *et al.* [1], and described in further detail elsewhere [12], so only a brief description is given here. The initial K-shell vacancy is produced by a 1634-eV electron beam. Hemispherical, electrostatic, energy analyzers are set to detect the Auger electrons and N^+ fragment ions of selected energies. Each analyzer shown in Fig. 1 can be moved in angle independently.

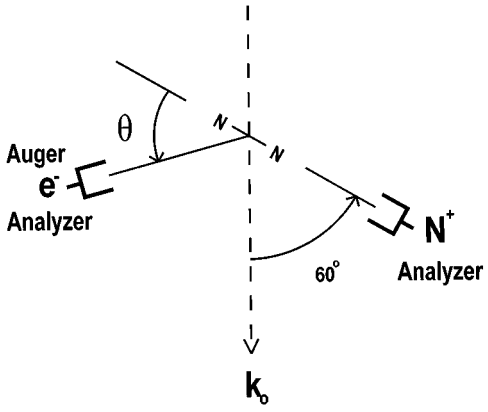

FIG. 1. Schematic diagram of the collision region. $\mathbf{k}_0$ represents the incident electron beam. The N^+ analyzer is fixed at 60°, while the electron analyzer is changed in angle. N^+-fragment ions are measured in coincidence with Auger electrons.

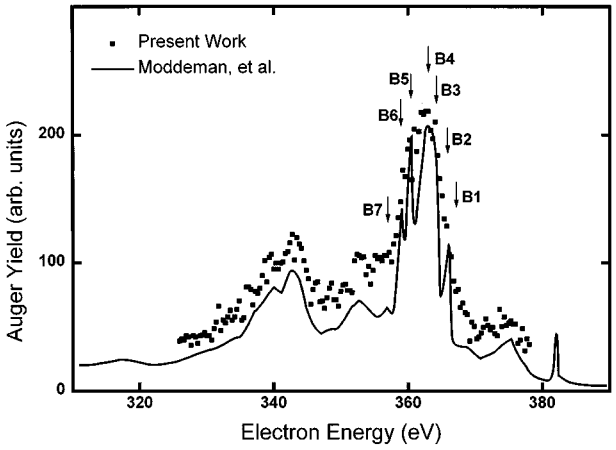

FIG. 2. Auger spectrum of N_2. Points are the present results and the line and labeling of the peaks is from Ref. [11].

The positive ion detector is set at 60° relative to the beam direction for all measurements, while the electron detector is placed on the opposite side of the beam and moved in angle. According to the axial recoil approximation, the N^+ fragments that are detected come from N_2 molecules aligned along the axis of the positive-ion analyzer. Therefore, the coincidence measurement yields the angular distribution of the Auger electrons emitted by the N_2 molecules with their internuclear axis at 60° relative to the beam direction. This angle was chosen for the N^+ detector because it allowed for measurements of the electron angular distributions over the range of 0°–90° relative to the internuclear axis.

To begin the measurements, the electron analyzer is placed at 90° relative to the beam direction (30° relative to the internuclear axis), and set to pass electrons of a selected energy (one of the peaks in the Auger spectrum of Fig. 2). Next, the voltages on the positive ion analyzer are stepped, as the energy is searched for the maximum in the coincidence count rate. Once the peak of the coincidence rate is found, voltages on the positive analyzer are set, and the electron analyzer is changed in angle to record angular distributions.

The Auger electrons or N^+ ions leaving the collision region pass through two slits that define the interaction volume for each analyzer. Particles that traverse the slits are focused onto the entrance of their respective analyzer by a zoom lens. The angular acceptance of the slits of each analyzer $\pm 1.5°$, as measured from the center of the interaction region. The angular placement of the analyzers can be set to better that 0.5°. Several runs were made at each angle as a means of checking for reproducibility and variations outside of statistical uncertainties. As the electron detector is moved in angle, that data must be corrected for (1) the variation in the beam length common to both detectors, and (2) the change of angular acceptance from each point along the common beam length. The procedure for doing this is described in Ref. [12].

The zoom lens located between the defining slits and the analyzer entrance allows for variation of the analyzing energy while maintaining a proper focus. The usual operating parameters of the hemispherical analyzers are energy resolutions of 1.5% for each, with the electrons analyzed at $\frac{1}{2}E_0$, and the N^+ ions analyzed at $10E_0$, where E_0 is the original energy of the electron or ion. However, several variations of these parameters were used in these measurements in order to optimize the collection efficiency.

The B-3 and B-4 transitions are separated by only 1 eV, whereas the electron energy resolution was 2.7 eV at this energy. In order to further attenuate coincidence contributions from B-4 in the B-3 measurement, the energy analysis of N^+ was decreased to $1.29E_0$. E_0 was 3.7 eV. It was possible to estimate the percentage contamination from this neighboring peak. The peak of the N^+ distribution was at 4.3 eV [1] for B-4, and its energy distribution was predicted from reflection approximation calculations. This yielded the relative intensity of N^+ ions 0.6 eV from the peak energy. Knowing the transmission function of each analyzer and the energy distribution of electrons and ions, we estimated the B-4 coincidence contribution to be about 12%. The B-2 transition does not end in a dissociative state, and, therefore, does not contribute coincidences.

The angular distribution of the B-5 transition at 360.2 eV was measured with smaller slits which reduced the energy resolution of both detectors to 1%. The electrons and ions were analyzed at the usual $\frac{1}{2}E_0$ and $10E_0$, respectively. This gave an energy resolution of the Auger electrons of 1.8 eV and, coupled with the energy analysis of the N^+ ions at 5.4 eV, the contribution from B-4 was considered negligible. If the transition at 358.7 eV (B-6) had been dissociative, it would not have been a contaminant because it should dissociate to different final states ($^1D + {}^1S$) than the B-5 transition and yield lower-energy N^+ ions. The energy acceptance of the N^+ analyzer would prevent coincidences from occurring.

III. THEORY

The angular distributions of the Auger electrons are predicted by solving the transition matrix elements in prolate spheroidal coordinates [2]. This requires knowledge of the bound-state and free-particle wave functions and a proper expansion of the interaction potential. Bound-state wave functions are found by solving the Schrödinger equation numerically with the aid of experimental values [13] of the energy of each orbital. A partial-wave expansion in prolate spheroidal coordinates is used for the ejected electron. The bound-state solutions are used to generate an effective potential that affects the outgoing Auger electron. This potential is used in solving the Schrödinger equation for the partial waves of the free particle.

Antisymmetric wave functions for a two-particle system are used to solve the two-particle transition moment. The interaction for the two electrons involved in the Auger transition is r_{12}^{-1}. The number of terms needed in the expansion of r_{12}^{-1} and in the partial-wave expansion are determined by convergence of the series expansions.

Three experimental factors broaden the predicted angular distribution. The axial recoil approximation is only good to first order, and some correction is necessary for rotational motion of the molecule. The shape of the potential-energy curve near the Franck-Condon region influences the amount of rotation during dissociation, so it is important to have reliable curves. Another broadening effect is due to the thermal translational motion of the molecule, and a third is due

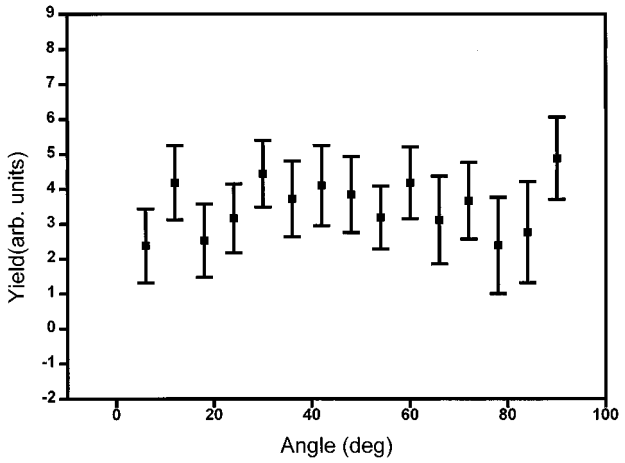

FIG. 3. Angular distribution of the 363.5-eV Auger electrons (B-3) relative to the internuclear axis.

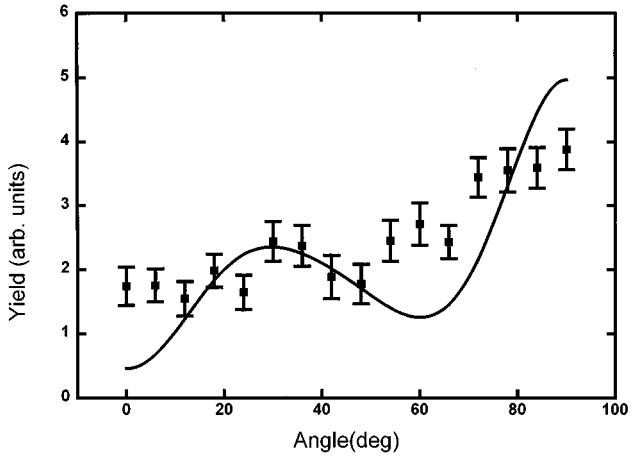

FIG. 4. Angular distribution of the 360.2-eV Auger electrons (B-5) relative to the internuclear axis. The line represents calculated values.

to the finite size of the slit system of the analyzers. The procedure for determining each of these corrections was described by Wood and coworkers [12,14]. Still another consideration is those states which dissociate by tunneling through a barrier. The molecular ions stays together for many rotations and, therefore, produces an isotropic angular distribution of Auger electrons in the laboratory frame.

IV. RESULTS

A. B-3 transition

The angular distribution of the Auger electron at 363.5 eV was found to be isotropic within statistical uncertainty (Fig. 3). Based on the theoretical potential-energy curves of O'Neil [8] and Wetmore and Boyd [5], it is assumed that the final state of this Auger transition is the $N_2{}^{2+}\,{}^1\Pi_u$ state. The Doppler-free measurements [10] of the N^+ spectrum show that several metastable vibrational states exist for the $^1\Pi_u$ with lifetimes against dissociation of a few hundred nanoseconds or less. These lifetimes lead to an isotropic angular distribution of the electrons in our measurements. Contamination from the nearby B-4 transition is not enough to disturb the isotropic distribution.

B. B-5 transition

The angular distribution of the 360.2-eV Auger transition (B-5) of N_2 and its calculated values are shown in Fig. 4. The yield is plotted as a function of the angle of emission relative to the internuclear axis. The error flags indicate statistical uncertainties only. The smearing of the distribution due to rotational motion and instrumental effects have been included in the calculated values.

The predicted angular distribution has been matched to the measured values by a single-parameter least-squares fit. There is only fair agreement between the calculations and measurements. The $^1\Pi_g$ ($2\sigma_u^{-1}1\pi_u^{-1}$ assumed configuration) potential-energy curve of Wetmore and Boyd [6] has been used to predict the angular distribution. There is no minimum in this potential curve, so the flatness of the measured distribution relative to the calculated values cannot be attributed to a metastable vibrational state. Possible explanations for the discrepancy are (1) the presence of an unresolved Σ state or, more likely, (2) limitations in the independent-particle model used to predict the angular distribution.

C. B-6 transition

No N^+ ions were found in coincidence with the Auger transition at 358.7 eV. It is assumed that the final state is the $^1\Sigma_u^+$ state of $N_2{}^{2+}$. This result is in agreement with the measurements of Eberhardt *et al.* [3], and the calculations of Olsson, Kindvall, and Larsson [7]. The potential-energy curve for the $^1\Sigma_u^+$ shows a fairly deep minima in the Franck-Condon region. If the doubly-ionized final state has a lifetime of several microseconds prior to dissociation then it can move out of view of the detector before separating into two fragments.

D. 3.9-eV N^+ peak

The N^+ kinetic-energy spectrum produced in collisions of fast projectiles with N_2 shows a maximum at 3.9 ± 0.2 eV [9,10,15,16]. In our experiment this peak has not been found to correlate with one of the strong (B-2$-$$B$-6) Auger transitions. An Auger transition to the $^3\Sigma_g^-$ state from either of the $1\sigma_g^{-1}\,{}^2\Sigma_g^+$ or $1\sigma_u^{-1}\,{}^2\Sigma_u^+$ inner-shell excited states is forbidden. However, the $^3\Sigma_g^-$ state is readily accessible by valence-shell ionization, and is believed to contribute to the 3.9-eV N^+ peak. This is supported by the potential-energy curve calculated by O'Neil [8], and Yousif, Lindsay, and Latimer [17], who predicted this identification based on the calculations of Wetmore and Boyd [6]. The earlier works of Edwards and Wood [9] attributed the maximum to the $^1\Pi_u$ state based on the calculations of Thulstrup and Anderson [4].

ACKNOWLEDGMENTS

This material was based upon work supported by the National Science Foundation under Grant No. PHY-9307129.

[1] Q. Zheng, A. K. Edwards, R. M. Wood, and M. A. Mangan, Phys. Rev. A **52**, 3940 (1995).
[2] Q. Zheng, A. K. Edwards, R. M. Wood, and M. A. Mangan, Phys. Rev. A **52**, 3945 (1995).
[3] W. Eberhardt, E. W. Plummer, I.-W. Lyo, R. Carr, and W. K. Ford, Phys. Rev. Lett. **58**, 207 (1987).
[4] E. W. Thulstrup and A. Andersen, J. Phys. B **8**, 965 (1975).
[5] Hans Ågren, J. Chem. Phys. **75**, 1267 (1981).
[6] R. W. Wetmore and R. K. Boyd, J. Phys. Chem. **90**, 5540 (1986).
[7] B. J. Olsson, G. Kindvall, and M. Larsson, J. Chem. Phys. **88**, 7501 (1988).
[8] S. V. O'Neil (private communication).
[9] A. K. Edwards and R. M. Wood, J. Chem. Phys. **76**, 2938 (1982).
[10] M. Lundqvist, D. Edwardsson, P. Baltzer, and B. Wannberg, J. Phys. B **29**, 1489 (1996).
[11] W. E. Moddeman, T. A. Carlson, M. O. Krause, B. P. Pullen, W. E. Bull, and G. K. Schweitzer, J. Chem. Phys. **55**, 2317 (1971).
[12] R. M. Wood and A. K. Edwards, *Accelerator-Based Atomic Physics Techniques and Applications*, edited by S. M. Shafroth and J. C. Austin (AIP, New York, 1997).
[13] K. Siegbahn, C. Nordling, G. Johansson, J. Hedman, P. F. Heden, K. Hamrin, U. Gelius, T. Bergmark, L. O. Werme, R. Manne, and Y. Baer, *ESCA Applied to Free Molecules* (North-Holland, Amsterdam, 1969).
[14] R. M. Wood, Q. Zheng, A. K. Edwards, and M. A. Mangan, Rev. Sci. Instrum. (to be published).
[15] F. Feldmeier, H. Durchholz, and A. Hofmann, J. Chem. Phys. **79**, 3789 (1983).
[16] H. Cho and S.-E. Park, Phys. Rev. A **51**, 1687 (1995).
[17] F. B. Yousif, B. G. Lindsay, and C. J. Latimer, J. Phys. B **23**, 495 (1990).